PERGAMON

Journal of Geodynamics 36 (2003) 169–191

JOURNAL OF GEODYNAMICS

www.elsevier.com/locate/jog

# Crustal architecture and active growth of the Sutai Range, western Mongolia: a major intracontinental, intraplate restraining bend

Dickson Cunningham[a,*], Sarah Davies[a], Gombosuren Badarch[b]

[a]*Orogenic Processes Group, Department of Geology, University of Leicester, Leicester LE1 7RH, UK*
[b]*Institute of Geology and Mineral Resources, Mongolian Academy of Sciences, Ulaan Baatar, Mongolia*

**Abstract**

The Sutai Range is a structural and topographic culmination at the southeastern end of the Mongolian Altai and a world-class example of an actively forming restraining bend. The range occurs at a major stepover zone along the Tonhil dextral strike-slip fault within a wider region dominated by late Cenozoic transpressional deformation. Analysis of satellite imagery and the results of field investigations reveal that the range is structurally asymmetric with an overall NE tilt due to several major SE-directed thrusts within the core of the range and along its SW margin. The distribution of alluvial sediments shed from the range and stream length asymmetries also indicate a regional NE tilt for the range. Faults that splay off of the main Tonhil Fault bound discrete uplifted blocks that define an oblique-slip duplex at the surface and asymmetric flower structure in cross-section. Outward growth of the range is partly accommodated by growth of foreberg thrust ridges within the adjacent Dariv Basin. Thrust blocks within the centre of the range expose basement schists and mylonitic granite suggesting that the greatest uplift and crustal exhumation has occurred within the core of the restraining bend, although much of the exhumation is likely to be due to older Palaeozoic structural events. The southeast and northwest ends of the range are characterized by smooth unbroken surface ramps (“gangplanks”) that are upwarped towards the centre of the range where maximum Cenozoic uplift has occurred. The geometry and evolution of Sutai Uul and other intracontinental and intraplate restraining bends is fundamentally influenced by the initial width of the stepover zone, the attitude of regional basement structures and extent of brittle reactivation, the direction of SHmax relative to basement structures, and progressive fault and block rotation which may change the kinematics along faults or lead to their abandonment.


* Corresponding author. Tel.: +44-116-252-3649; fax: +44-116-252-3918.
*E-mail address:* wdc2@le.ac.uk (D. Cunningham).

0264-3707/03/$ - see front matter © 2003 Elsevier Ltd. All rights reserved.
doi:10.1016/S0264-3707(03)00046-2

## 1. Introduction

This report concerns the geology and structural evolution of the Sutai range in western Mongolia (Fig. 1) which is a world-class example of an actively forming restraining bend. Restraining bends are discrete mountain ranges that occur at transpressional stepover zones between en echelon segments of strike-slip faults or at contractional strike-slip termination zones (Crowell, 1974; Biddle and Christie-Blick, 1985). They are typically high, but narrow ranges containing uplifted basement rocks in their cores and bounded by thrust and oblique-slip faults that link with the strike-slip fault(s) that enter the range. Thus they are active sites of mountain building and also mountain erosion which commonly leads to alluvial basin development adjacent to the range. Fault geometries within restraining bends typically define positive flower structures (usually asymmetric) and plan-view fault trends may define a strike-slip duplex pattern (Biddle and Christie-Blick, 1985; Woodcock and Fisher, 1986). Restraining bends are an important mountain range type that occur along transform boundaries or in intraplate, intracontinental strike-slip and transpressional settings. Previously described examples include the Transverse and Santa Cruz Ranges in California (Crowell, 1979; Blythe et al., 2000; Anderson, 1990; Schwartz et al., 1990), the Blue Mountains, Jamaica (Mann et al., 1985), Hispaniola (Mann et al., 1984), the Lebanon Range (Butler et al., 1998), Turkish ranges (Barka and Kadinsky-Kade, 1988),

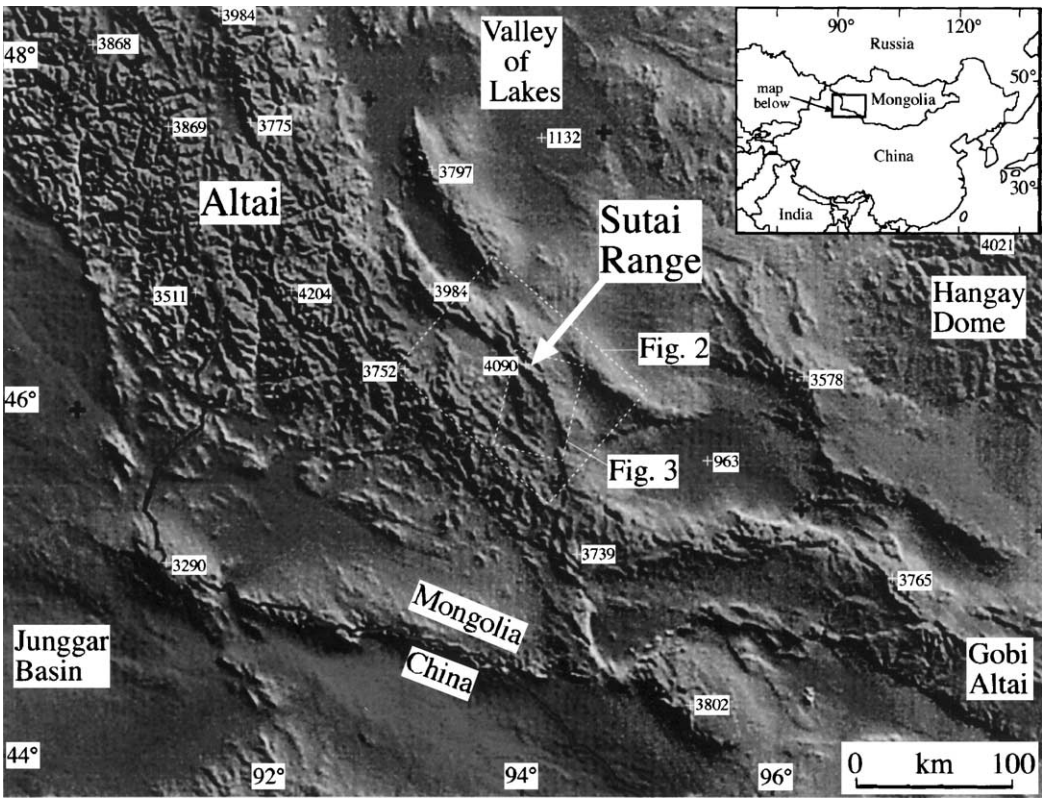


Fig. 1. Digital topographic map of the southeastern Altai region in western Mongolia. Location of Sutai range which is a structural and topographic culmination at the southeastern end of the Altai is shown as is location of Figs. 2 and 3.

Cordillera Darwin, Chile (Cunningham, 1995), and the northern Gobi Altai in Mongolia (Cunningham et al., 1996a; Bayasgalan et al., 1999).

Understanding the evolution of restraining bends and controls on their distribution is important for several reasons: (1) they commonly are sites of earthquake rupture nucleation or along-strike rupture impedance, and thus directly influence the seismic hazard in a region (e.g. Barka and Kadinsky-Kade, 1988; Kadinsky-Kade and Barka, 1989; Legg, 2000). Some major cities lie adjacent to restraining bends (e.g., Los Angeles, Beirut, Guatemala City) and are directly affected by active seismicity associated with restraining bend growth; (2) they expose basement rocks that may contain economic resources; (3) they provide a window into the crystalline basement which in some localities is the only source of information on the early crustal evolution of a region; and (4) they are excellent natural laboratories for studying the relationship between faulting, topographic uplift and alluvial sedimentation and for understanding the linkage and partitioning of strain between faults with different kinematic histories (e.g. Laney and Gates, 1996).

Few detailed studies exist which attempt to describe the structural evolution and internal architecture of an actively forming restraining bend. The issue is complex because dating fault formation, progressive displacements and eventual fault abandonment is difficult. Geomorphological features such as fault scarps, raised terraces, and alluvial fan deposits, can provide information on relative timing of fault activity, but in most cases, do not elucidate the earlier stages of restraining bend nucleation and development. Therefore, analogue modelling is particularly useful for examining the possible spatial and temporal growth of a restraining bend. For example, Keller et al. (1997) showed that a singular restraining bend generally develops by linkage of P-shears between strike-slip segments which progressively accommodate contractional and oblique-slip movements. Their experiments also demonstrated that vertical-axis rotation of fault-bounded blocks occurs within the bend during progressive shearing. McClay and Bonora (2001) carried out various analog models of restraining bend evolution with different strike-slip fault overlap relations and documented the development of flower structure fault geometries and oblique-slip motions within the bend. By combining an inventory of natural examples at different stages of development with study of analogue models, we stand the best chance of understanding how restraining bends originate and progressively develop.

In this paper, we combine remote sensing analysis of Kosmos and space shuttle imagery with structural and geomorphological investigations to better define the fault architecture, neotectonic activity and overall crustal development of the Sutai Uul restraining bend in western Mongolia. We focus on the southern and eastern parts of the range where the active Tonhil strike-slip fault enters the range (Figs. 2 and 3) and where access and exposure are best. We propose an evolutionary model for the range which is consistent with image and field observations and which may apply to other transpressional orogens.

## 2. Cenozoic tectonics of western Mongolia

The Sutai range is located along the southeastern edge of the Mongolian Altai in southwestern Mongolia (Fig. 1). The Altai is one of the great Cenozoic ranges of central Asia stretching over 1700 km in length from Siberia to the Gobi Desert. Elevations reach 4506 m with dozens of other summits exceeding 4000 m and permanent snow and glaciers generally above 3700 m. The range

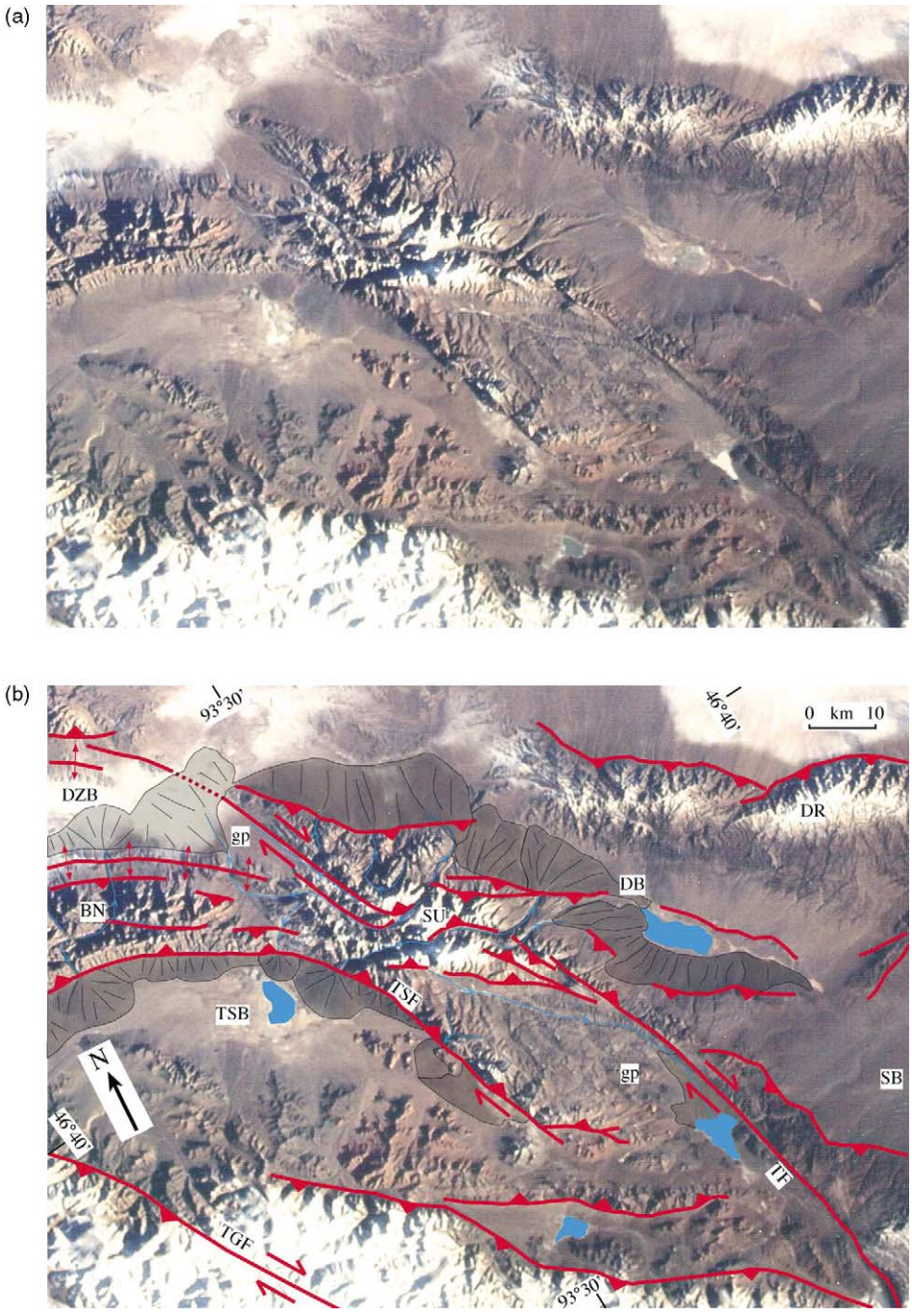


Fig. 2. (a) Space shuttle view of Sutai Uul and surrounding ranges. See Fig. 1 for location. (b) Interpretation of image showing major faults, sites of Late Cenozoic alluvial deposition from Sutai range (shaded), and overall active tectonic setting within dextral transpressional deformational regime in southeastern Altai region. SU: Sutai Uul; BN: Baataryn Nuruu; DR: Dariv Range; DZB: Dzereg basin; DB: Dariv Basin; SB: Shargan Basin; TSB; Tsetseg Basin; TF: Tonhil Fault; TSF: Tsetseg Fault; TGF: Turgin Gol Fault; gp: ''gangplank''—an unbroken topographic ramp — see text for discussion.

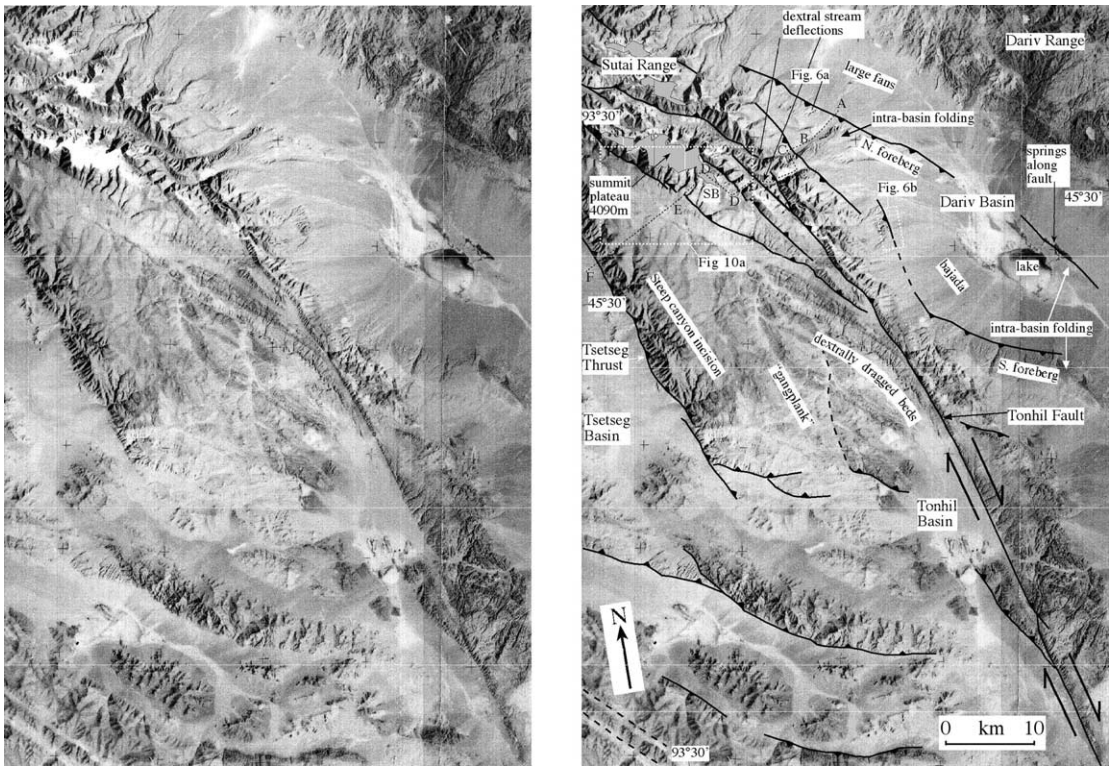


Fig. 3. (a) Kosmos image of Sutai Uul restraining bend, Tonhil Fault and surrounding areas. See Fig. 1 for location. (b) Interpreted image showing major faults, and geomorphological features. A–F corresponds to geological transect discussed in report and shown in Fig. 8. SB: Summit Block.

is tectonically active and has experienced numerous historic earthquakes with several $M>7$ (Khil'kho et al., 1985, and Baljinnyam et al., 1993; Bayasgalan et al., 1999). Active faults are found throughout the Altai and are typically NW-striking thrust faults and dextral strike-slip and oblique-slip faults defining an overall transpressional regime (Cunningham et al., 1996b, 2003). Maximum horizontal stress in the region is northeasterly based on historic earthquake mechanisms (Zoback, 1992). The Mongolian Altai is dominated by discrete block uplifts bounded by active faults that commonly define asymmetric flower structures. On the eastern margin of the Altai, isolated ranges are separated by alluvial basins (Fig. 1), whereas further west, discrete transpressional blocks have grown laterally and have coalesced to define a topographically continuous range (Cunningham et al., 1996b, 2003).

The geomorphology of the Altai reflects its youthful nature. Many summits preserve a late Cretaceous-Palaeocene peneplane and many ranges are tilted blocks with asymmetric drainage patterns (Cunningham et al., 2003). Active fault scarps cut Quaternary deposits along numerous regional fault systems and intramontane basins with fresh alluvial deposits bound many ranges. An Oligocene unconformity in basins along the eastern margin of the Altai marks the onset of renewed tectonism in the Mongolian Altai (Devyatkin, 1981; Howard et

al., 2003). Reactivation of the Altai is believed to be due to NE-directed horizontal compressive stresses derived from the distant Indo-Eurasia collision over 2000 km to the south (Tapponnier and Molnar, 1979; Baljinnyam et al., 1993; Cunningham et al., 1996b, 1988, 2003).

## 3. Basement geology of western Mongolia

The basement geology of the Altai records a complex history of Palaeozoic terrane accretion and arc magmatism. The range is within the Central Asian Orogenic Belt which is defined as the wide belt of juvenile Phanerozoic continental crust that formed between the older Siberian, Tarim and North China cratons (Mossakovsky et al., 1994). Distinctive terranes have been recognized which are either Precambrian continental fragments, Palaeozoic subduction complexes or Palaeozoic arc and back-arc complexes (Chen and Jahn, 2002; Windley et al., 2002; Badarch et al., 2002). Post-orogenic intrusive rocks occur widely throughout the range (Gavrilova, 1975).

The Mongolian Altai has experienced a polydeformational history with most basement metamorphic complexes demonstrating at least two stages of ductile contractional deformation, as indicated by multiple fold generations and cleavage relationships. The overall basement structural grain is generally NW-striking and NE-dipping and most basement folds and shear zones suggest SW-directed folding and thrusting during the lower Palaeozoic (Cunningham et al., 1996b, 2003). Post-orogenic extensional shear zones occur in discrete belts within the core of the range, however the regional significance of these zones is not yet well understood (Cunningham et al., 1996b, 2003; Windley et al., 2002). Mesozoic contractional tectonic activity is recorded in the neighbouring Tien Shan (Hendrix, 2000; Dumitru et al., 2001), but not yet documented in the Altai. Mesozoic clastic sequences occur in basins along the eastern margin of the Mongolian Altai such as the Dzereg and Dariv basins (Fig. 2) and may be related to a localized rifting event in the Jurassic-Cretaceous (Howard et al., 2003; Sjostrom, 2001).

### 3.1. Bedrock geology of the Sutai range

The oldest rocks of the Sutai range are greenschist-grade slates, phyllites and schists that occur in the eastern half of the range and that represent metamorphosed volcaniclastic sediments and volcanic rocks (Fig. 4). These units are regionally correlated with Vendian-Cambrian rocks found extensively throughout the Mongolian Altai (Zaitsev, 1978). Ordovician-Silurian greenschist grade metasedimentary and metavolcanic rocks occur in the western part of the range and include deformed pillow basalts, marble, and chlorite-quartz phyllites. Undated granitic intrusives cut the basement rocks throughout the range. The basement metamorphic and intrusive rocks are unconformably overlain by undated volcanic rocks, Carboniferous clastic rocks including coal-bearing sequences, and Jurassic coarse conglomerates (Zaitsev, 1978). The large volumes of volcanic, volcaniclastic and intrusive rocks within the range suggest that the basement is dominantly a Palaeozoic volcanic arc assemblage possibly developed on an accretionary complex.

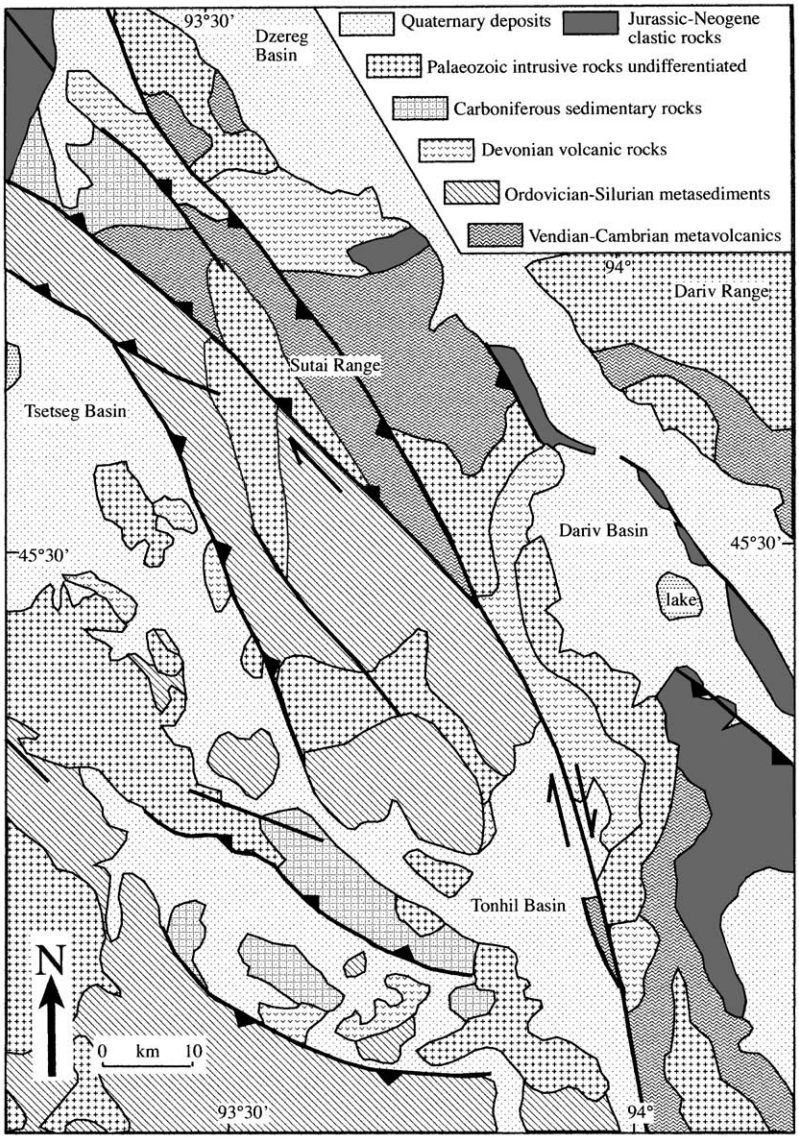


Fig. 4. Geological Map of Sutai Range and surroundings, western Mongolia (adapted from Zaitsev, 1978).

## 4. Remote sensing analysis of the Sutai range

A large amount of information concerning the active faulting and tectonic geomorphology of the Sutai range and surrounding basins is evident from the Kosmos and space shuttle images (Figs. 2 and 3). The Tonhil fault is expressed as a sharply defined linear trace that curves gently towards the northwest as it enters the range from the south. Dextral sense of motion is indicated by dragged lithologic belts and two prominent stream valley offsets in the north (Fig. 3). The eastern side of the Tonhil fault is an uplifted ridge, suggesting a minor east-side-up reverse component of motion has

also occurred along the length of the fault. This reverse component of displacement must increase towards the north to account for the northwards increase in elevation of the ridge on the east side of the fault (Figs. 2 and 3). Two northwest-striking, sharply defined fault zones that bound the Sutai summit block splay off of the Tonhil fault (Fig. 3). Topographic offsets across these faults suggest that they are northeast dipping thrusts. Several other sharply defined fronts and valleys within the range at the northern end of the Tonhil Fault suggest that they are also active splays (Fig. 3).

The western boundary of the range is the Tsetseg thrust fault (Figs. 2, 3 and 5b) which is an active northeast-dipping thrust previously reported by Cunningham et al. (1996a). The western range front has low sinuosity and large fresh alluvial fan complexes which locally preserve a degraded fault scarp that cuts the fans (Fig. 5b). The steep relief along the front and presence of short, but deeply incised canyons also suggest recent fault activity. The southern extent of the Tsetseg Fault may also have a dextral strike-slip component as it is parallel to the dextral Tonhil and Turgin Gol Faults (Fig. 2).

Deformation of the Dariv Basin sedimentary fill is evident on the images (Figs. 2 and 3). Two prominent NW-trending forebergs cut into the basin and are bounded by northeast-directed thrusts and contain internally folded Mesozoic-Cenozoic basin fill (Figs. 3 and 6a). A small NNW-trending ridge and line of springs occurs within the basin east of Dariv Lake which marks a fault zone that may link the two foreberg thrusts (Fig. 2). A small degraded thrust scarp is also visible on the west slope of the Dariv Basin (Figs. 3 and 6b).

The Kosmos image shows a remnant summit plateau which is snow and ice-capped and preserved on three main ridge tops (Figs. 3 and 5a, b). Deep canyon incision around these plateau remnants suggests high rates of topographic uplift within the core of the Sutai range.

The Kosmos image also shows areas that are relatively unaffected by Cenozoic tectonism or are simply regionally tilted. Several small ranges at the southern end of the image have high mountain front sinuosity and mature eroded landscapes. They contrast with several thrust bounded ridges which are sharply defined and marked by canyon and gully incision (Fig. 3). The Dariv Range also lacks evidence for an active range front on its SW side and is onlapped by large alluvial fans from the Sutai range at the northern end of the Kosmos and shuttle images (Figs. 2 and 3). The main axial drainage that runs into Dariv Lake is shifted far to the northeastern side of the basin as a result. The southern end of the Sutai range is a regionally SSE tilted surface labelled ''the gangplank'' (Figs. 2 and 3) because it is a gentle topographic ramp which appears to be largely unbroken by Cenozoic faults. A small river flows down this regionally tilted surface towards the small and isolated Tonhil Basin depocentre (Figs. 2 and 3). Small southwest-directed thrust splays at the southeastern end of the Tsetseg thrust, to the west of the Tonhil Basin, and along the Tonhil Fault SSE of the Tonhil Basin appear to be propagating towards each other and may eventually link and disrupt this ''gangplank'' surface (Fig. 3).

The space shuttle image of the range is lower resolution than the Kosmos image, but shows other important regional features (Fig. 2). The distribution of sediments eroded off of the Sutai range indicates that most sediment is deposited as alluvial fan and bajada complexes to the NE or SW in front of bounding thrusts. More sediment appears to be deposited in the Dariv and Dzereg basins than along the SW side in the Tsetseg Basin. In contrast, the centre of the Tsetseg basin appears sediment starved whereas prominent alluvial fan complexes are developed along the Sutai and Baataryn Nuruu front adjacent to the gently curving Tsetseg thrust fault (Fig. 2). The

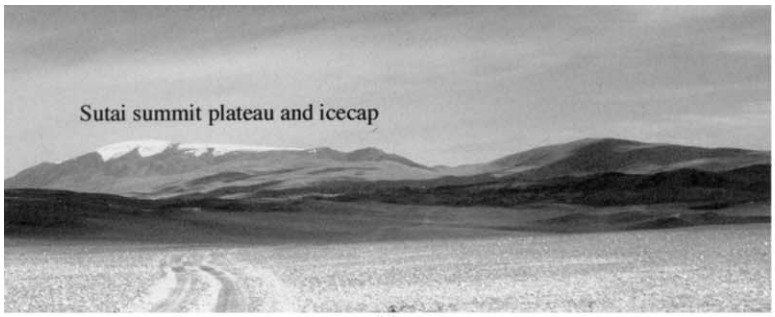


(a)

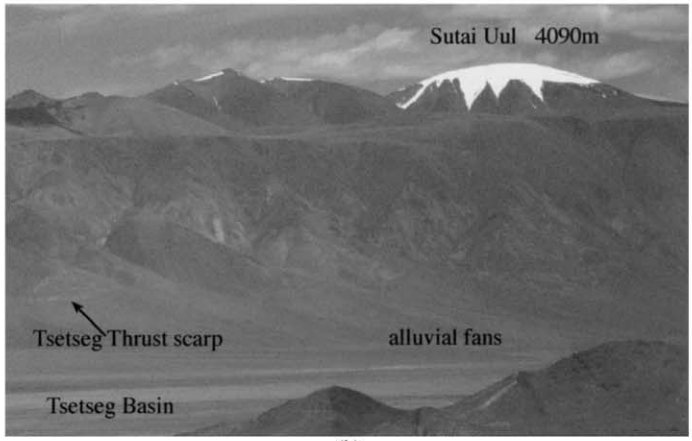


(b)

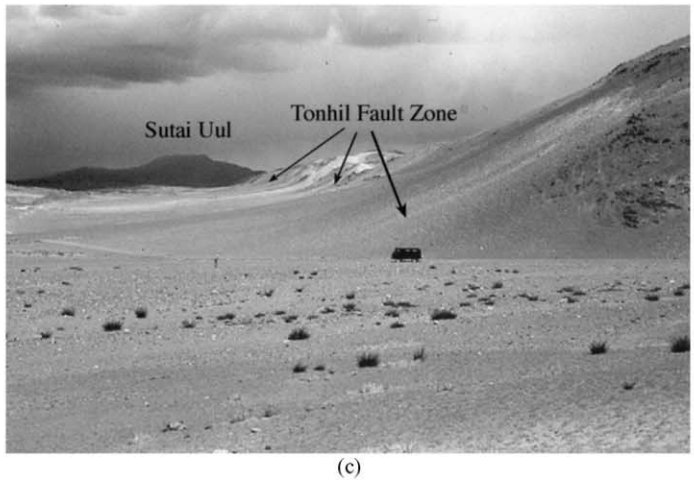


(c)

Fig. 5. (a) View from S towards Sutai summit plateau and icecap. View is up the so-called ''gangplank'' which is a relatively smooth unbroken surface that is tilted upwards to the north towards the summit block (Figs. 2 and 3). (b) View looking E from Tsetseg Basin at bounding thrust scarp and fresh alluvial fan complex bordering Sutai range. (c) View from edge of Tonhil Basin looking NNW along Tonhil fault zone and distant Sutai range which lies at the transpressional termination zone for the fault system.


(a)

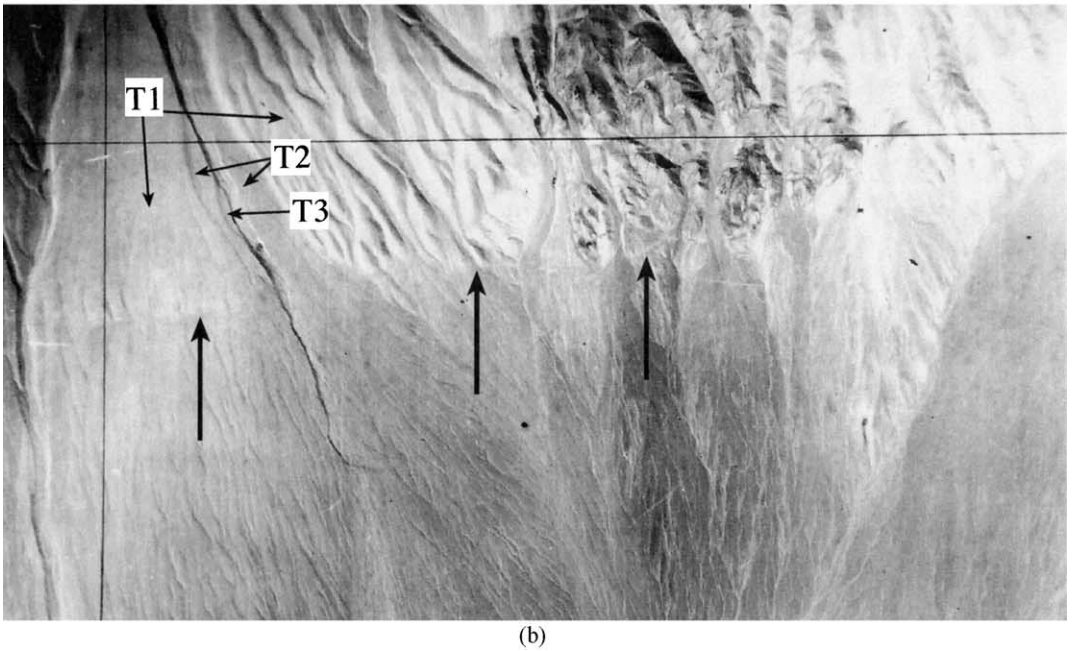


(b)

Fig. 6. (a) Photo looking N of folded Mesozoic-Tertiary basin sediments within thrusted northern foreberg on west side of Dariv Basin. Width of photo along skyline is approximately 300 m. (b) Aerial photo of degraded thrust scarp along western side of Dariv Basin. T1-T3 = ephemeral stream terraces with T1 being the oldest. See Fig. 3 for location of photos.

Dariv Basin fans are deflected around the northern and southern forebergs and the Dariv lake is ponded between the fan fronts and the small fault bounded ridge that runs northwesterly down the centre of the basin (Figs. 2 and 3). Major streams that supply the alluvial fan complexes have incised steep narrow canyons in the core of the Sutai range and most depart the range to the N, NE, or E suggesting bulk regional NE tilting. This is supported by the observation that most faults within the range that are visible on the images appear to be NE dipping, SW-directed thrusts and oblique-slip thrusts.

The northern end of the range contains two prominent linear fault zones which curve towards the east in the centre of the range. These faults are interpreted to be dextral faults that enter the range from the north, similar and parallel to the Tonhil fault which enters the range from the south (Fig. 2). They terminate as curved traces with increasing reverse displacements which have elevated the high snow-capped ridges in the northern part of the range. These faults bound a smooth valley surface that is tilted upwards towards the south, suggesting that it is a similar ''gangplank'' surface as is found adjacent to the Tonhil fault at the southern end of the range (''gp'' in Fig. 2).

The overall fault pattern visible in both images suggests that the Sutai Range is a double restraining bend developed between en echelon left-stepping segments of the dextral Tonhil fault system. The highest elevations occur at the stepover zone where thrusts and oblique-slip faults (essentially large P shears) splay off of the main strike-slip faults and accommodate uplift. The range appears to have a bulk northeastwards tilt based on stream length asymmetries, the large amount of sediment deposited to the N, NE and E in adjacent basins and the predominance of NE-dipping thrusts within the range. The low sinuosity and steep relief along the Tsetseg Fault suggest that it may be the most active thrust in the range and certainly more active than the faults that bound the eastern and northeastern range front. The Baataryn Nuruu also appears to be tilted northeastwards based on stream length asymmetries suggesting that the Tsetseg Fault is the dominant range bounding structure there also (Fig. 2).

## 5. Geological transects

Several cross-strike structural transects were made across different sectors of the range along line A–F in Fig. 3. At the northeastern end of the line (A), the thrust that bounds the NE foreberg margin is not exposed, but is inferred because of the abrupt topographic break on the northeast edge of the foreberg (Fig. 3), and uplifted and folded Cretaceous and Tertiary clastic rocks within the foreberg (Fig. 6a). The bounding thrust zone for the northeastern margin of the Sutai range is exposed in Section B–C about a kilometre out from the main topographic break that defines the range front (Fig. 7). At this location, heavily brecciated and altered granodiorite is thrust over a boulder conglomerate which is folded into a tight syncline immediately beneath the thrust. A small thrust slice of the granodiorite is repeated beneath the conglomerate. This slice overthrusts red silts which in turn are thrusted over brown and grey fanglomerates of Quaternary age. The thrust faults that cut the fanglomerates are carbonate cemented and stand out as white cemented fault planes which presumably were conduits for carbonate-rich fluids (Fig. 7).

Segment C–D (Fig. 3) covers much of the interior of the range and can be divided into discrete fault-bounded block domains (Fig. 8). At the northeast range front, a poorly exposed thrust zone

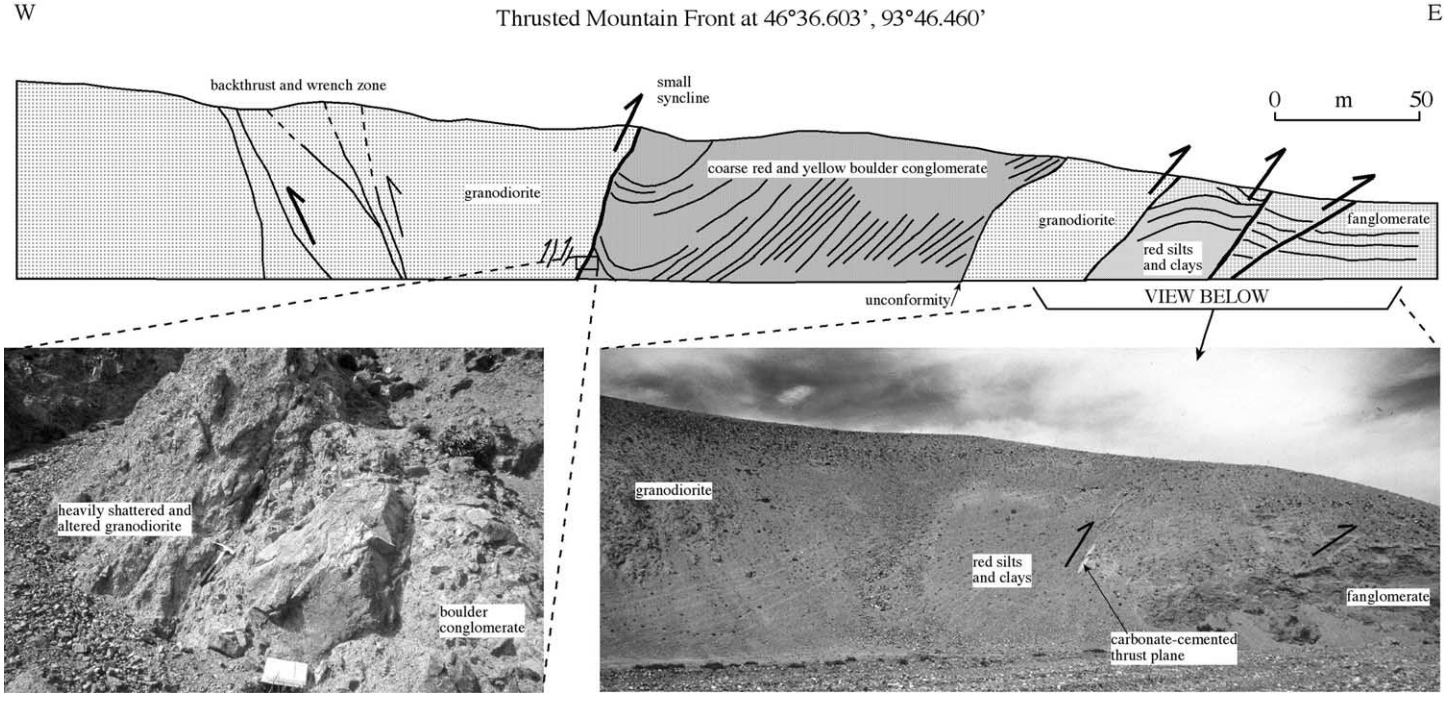


Fig. 7. Structural section of thrust front along eastern side of Sutai range. Section corresponds to transect segment B–C in Fig. 3. Two separate thrust faults place granodiorite over basin fill.

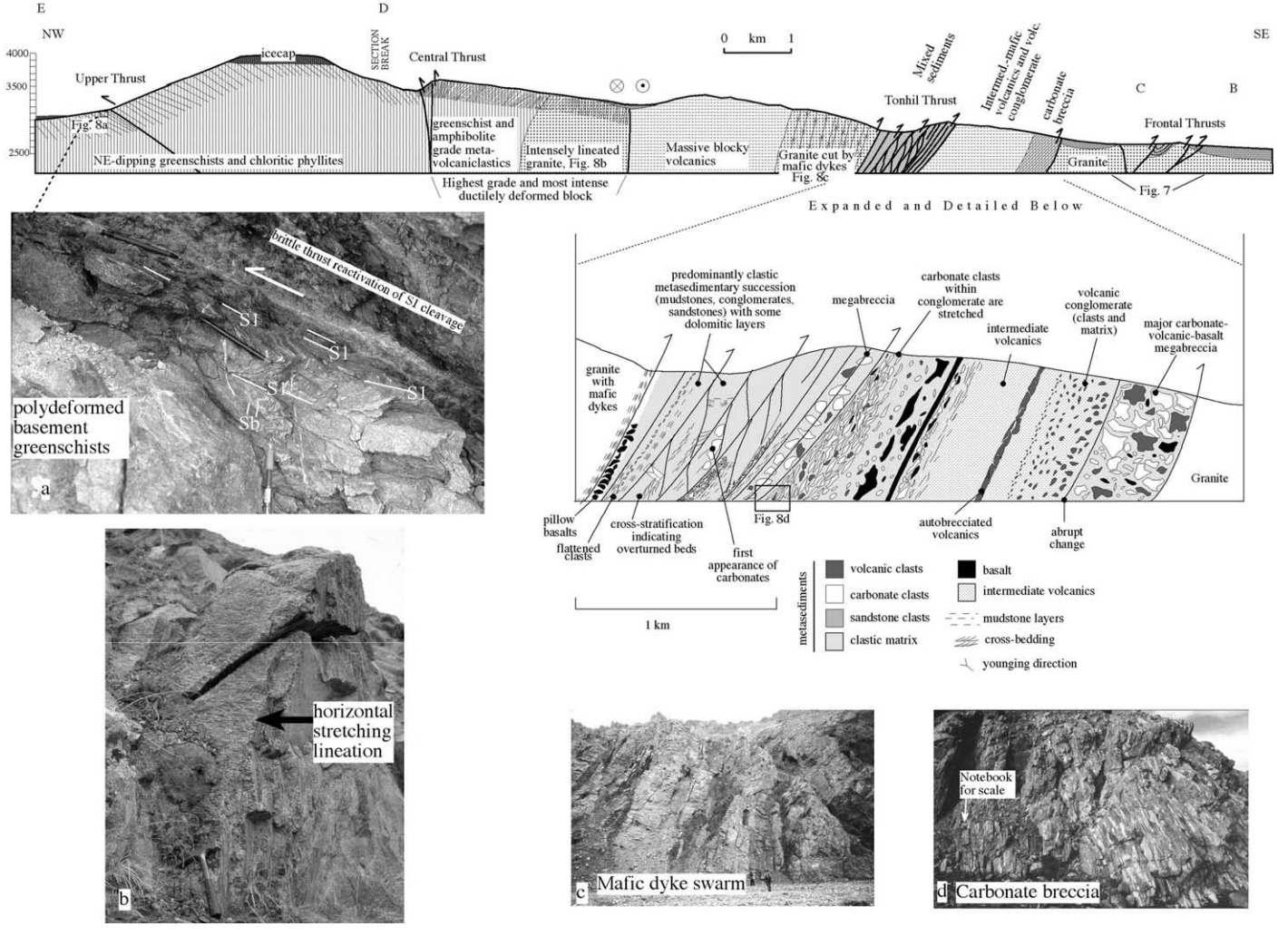


Fig. 8. Structural transect across eastern half of range corresponding to line B–E in Fig. 3. (a) Evidence for three stages of deformation recorded in basement greenschists near Upper Thrust on west side of summit block. Volcaniclastics contain sedimentary layering (Sb) which is tightly to isoclinally folded and transposed by a dominant S1 cleavage which is also locally folded. Both are cut or reactivated by brittle thrusts related to Cenozoic uplift of the range. (b) Strongly developed quartz and biotite stretching lineation within granite in core or range. Lineations are subhorizontal and rock is dominantly an l-tectonite. (c) Mafic dyke swarm which cuts granite within core of range. (d) carbonate megabreccia below Tonhil thrust.

places carbonate breccias and highly fractured andesites and volcanic conglomerates over the granodiorite. These units are steeply NE dipping to steeply SW dipping and overturned. They are in turn structurally below another major overthrust zone that is linked along strike to the Tonhil Fault (Fig. 3) and is thus named the Tonhil Thrust. This thrust zone places a granite complex that is notable for containing abundant parallel SW dipping mafic dykes over a mixed sedimentary sequence (Fig. 8c). The overthrusted sedimentary sequence contains greenish sheared mudrocks, green volcaniclastics, chloritic fault phyllites, dolomitized limestones, limestone breccias and conglomerates, purple siltstones and sandstones, and sheared conglomerates dominated by purple siltstone clasts. Sedimentary bedding is moderately to steep SW dipping (45–90°) and facing indicators including cross bedding suggest the sequence is overturned. Shear fabrics are widespread and consistently indicate top to the northeast thrusting (Fig. 9). Lineations indicate a subordinate dextral strike-slip component to the displacement (strike and dip of shear fabric: 322, 52SW, lineation: 48°, 222).

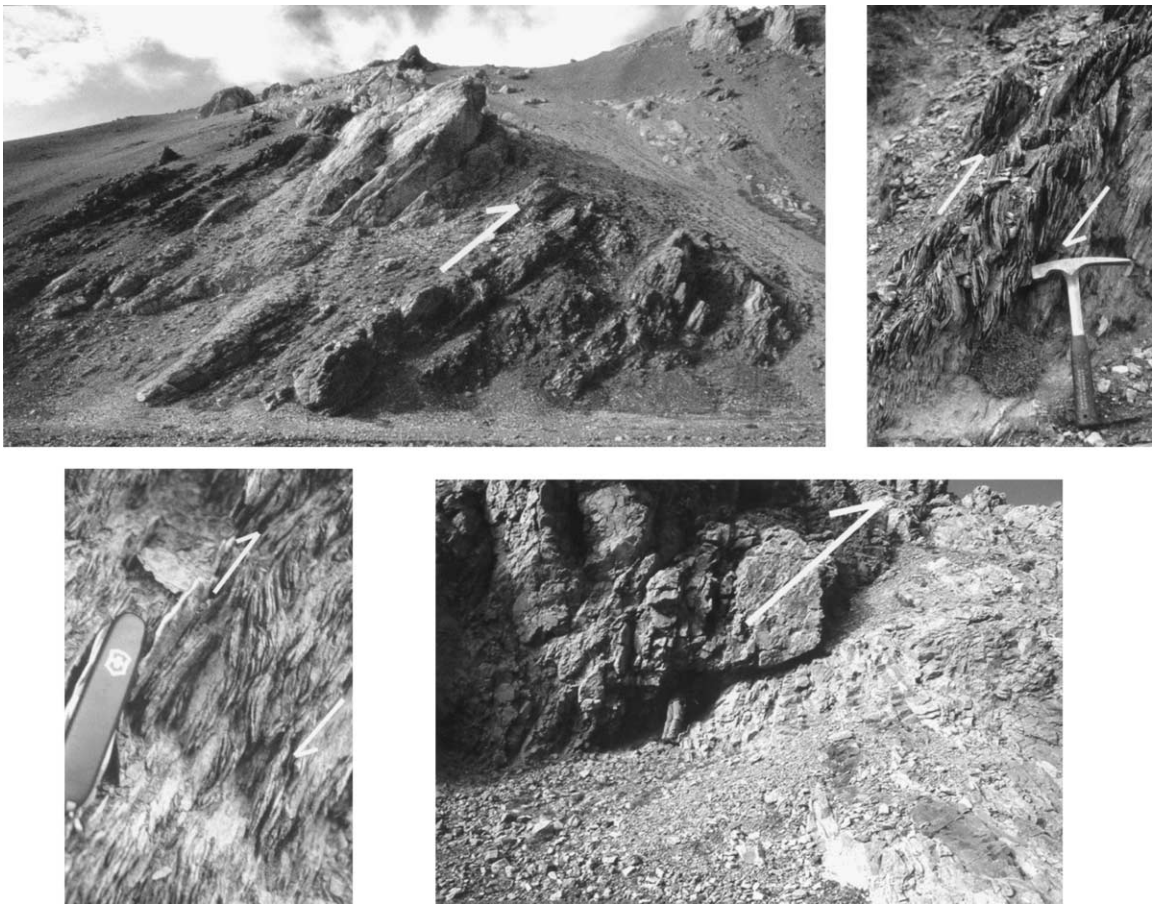

Fig. 9. Photos looking N of Tonhil thrust zone. See Fig. 8 for location. Fault zone dips west and places a granitic complex over a mixed sedimentary sequence containing sheared mudrocks (with well developed S–C fabrics), and brittley thrusted carbonates, carbonate breccias and volcaniclastic rocks (see detailed section in Fig. 8).

Further upslope, the granite intrudes a massive volcanic sequence on its western margin. These volcanic rocks range from rhyolitic to basaltic and are pervasively brittley fractured over a kilometer width. The fractures are generally steep to vertical and define an overall steep fracture "fabric". The western boundary to the volcanic sequence is a major linear valley that is the along-strike continuation of the main Tonhil dextral strike-slip fault (Fig. 3). The valley bottom is filled with talus and stream gravel and the fault is not exposed.

The Tonhil Fault is an important tectonic boundary that separates unmetamorphosed brittley deformed volcanic rocks on the northeast side from intensely ductiley deformed granite to the southwest. The granite intrusion west of the fault is mylonitic and contains a very strong quartz stretching lineation that in general, is better developed than the foliation. The foliation dips moderately SW to vertical (292, 90) whereas the lineation is consistently horizontal to shallowly NW or SE plunging (Fig. 8b). The rock is thus dominantly an L-tectonite, however sense of shear is ambiguous despite the strong lineation. Nevertheless the pervasive and penetrative sub-horizontal lineation suggests that a ductile strike-slip zone of unknown age occupies the deep core of the range.

The granite is grey to pinkish in colour and was observed to irregularly intrude meta-volcaniclastic rocks in high valley wall exposures. Rocks directly southwest of the granite are poly-deformed volcaniclastic sediments that contain refolded folds of bedding and a strong southwest dipping metamorphic fabric that locally appears to define outcrop-scale top-to-the northeast thrust duplexes. This fabric is generally axially planar to small isoclinal folds of the primary bedding. The rocks are generally schistose and contain amphiboles that define a moderately plunging NW trending lineation (S1 cleavage: 328, 55SW, with hornblende lineation: 44°, 299). These schists and the strongly lineated granite that intrudes them comprise the highest grade and most intense ductiley deformed rocks observed within the Sutai range.

These central schists are bounded to the southwest by a major fault zone that is well defined on the Kosmos image as a linear fault-bounded valley (Fig. 3). Close examination of the image indicates that the fault consists of en echelon left-stepping segments (Figs. 3 and 10a). In the field, the main fault is concealed by valley fill, however, small steep NE-dipping brittle faults were observed in the adjacent wall rock on the northeast side of the fault and small, asymmetric SW-vergent steeply SE-plunging kink folds are abundantly developed in green phyllites in the centre of the valley on the fault's southwest side. These minor kink folds suggest strongly that the main fault is a SW-directed thrust fault herein named the "Central Thrust" (Fig. 10a). The steep SE plunges for the kink-fold axes may suggest a dextral component of displacement accompanied thrusting. This fault zone cuts directly across the main SW-dipping fabric in the upper plate, whereas, it appears to be approximately fabric parallel to the NE-dipping lower plate phyllites (Fig. 8).

The Central Thrust forms the eastern boundary to a wide belt of monotonous NE-dipping green chloritic schists, phyllites and slates. Clasts and fragments within many layers indicate a volcaniclastic protolith for most of the metamorphosed sequence, although some greenstone sequences suggest metavolcanic protoliths and thin carbonate and calc-silicate layers occur locally. The rocks are less schistose and lower grade than the amphibole bearing schists NE of the Central Thrust. The main fabric typically dips shallowly to moderately northeastwards and no large-scale folds of the cleavage were observed. Primary bedding is tight to isoclinally folded and the main cleavage is axially planar to F1 folds of the bedding (Fig. 8a). This wide belt of

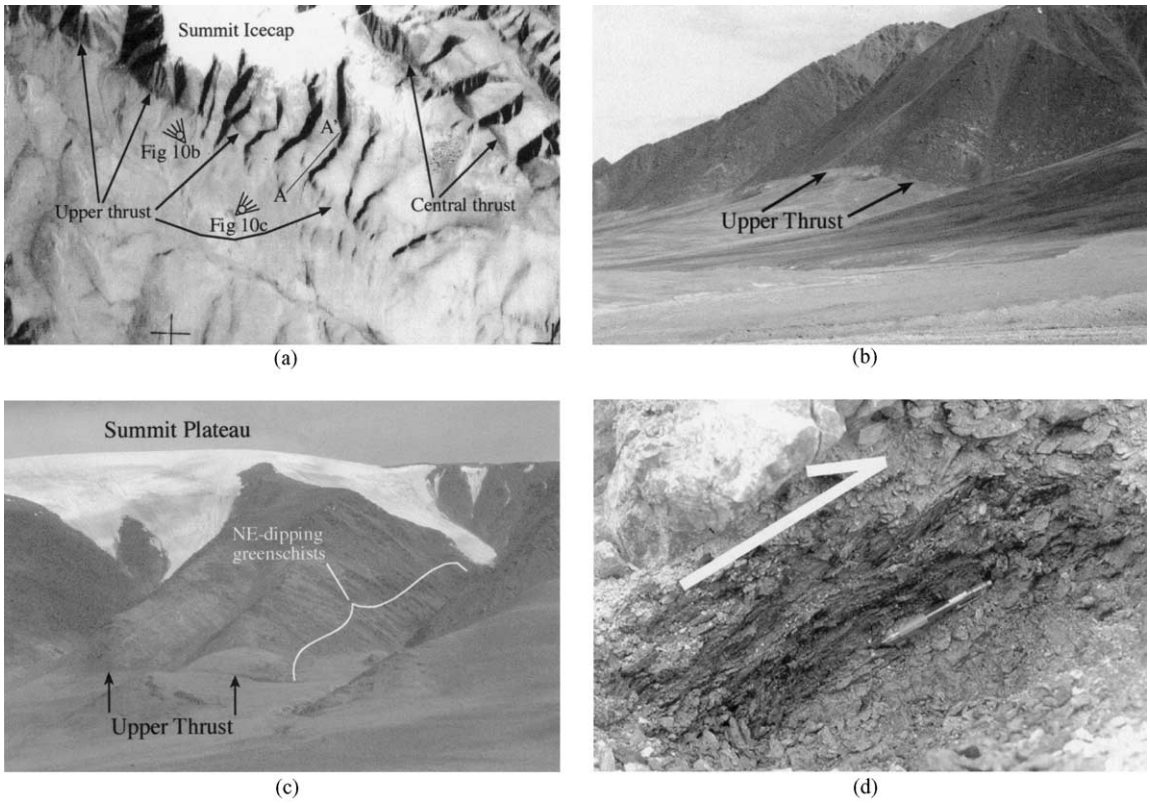


Fig. 10. (a) Kosmos image closeup of thrust faults that bound summit block. Both the Upper Thrust and Central Thrust dip NE and have uplifted greenschist and amphibolite grade metavolcanic and metavolcaniclastic basment rocks that represent the deepest rocks to have been exhumed within the range. Location of photo shown in Fig. 3. (b) View looking N of Upper Thrust which is marked by abrupt break in slope and steep relief at thrust front. Viewpoint is indicated in Fig. 10a. (c) View looking E of summit block and thrust front. Note visible fault scarp, homoclinal NE dipping greenschist sequence and summit plateau. Viewpoint is indicated in Fig. 10a. (d) Close-up of brittle shear fabrics with thrust sense kinematics within excavated exposure of Upper Thrust at 46°36.100, 93°35.930.

NE-dipping greenschist grade metavolcaniclastic rocks makes up the summit block to the range (Figs. 8 and 10c) and is a common basement succession found throughout much of the southern Mongolian Altai region (Cunningham et al., 1996b, 2003).

The summit block is bounded on its SW side by a major thrust zone called the ''Upper Thrust'' that marks a prominent break in slope and that is well defined on satellite imagery (Figs. 2, 3 and 10a–c). The steep western slope of the summit block is inclined 40° or more and steep canyons containing glaciers derived from the summit icecap have cut deeply across the thrust zone. The thrust zone is locally exposed, despite abundant talus debris and consists of a highly sheared zone of fault schists and phyllites with abundant phacoidal flakes which are well lineated (Fig. 10d). The shear fabric strikes 280, 34 NE with slickensides plunging 31°, 060. This slickenside attitude suggests that thrusting was accompanied by a minor sinistral strike-slip component of displacement. Below this major thrust zone, numerous minor brittle thrust faults were observed that have reactivated the main northeast-dipping metamorphic fabric (Fig. 8a).

## 6. Other field observations

### 6.1. Tonhil Fault

This major structure is marked by a prominent break in slope at the base of a small uplifted ridge which creates about 100 m of relief (Fig. 5c). In general, we found that the fault is poorly exposed and marked by discoloured rusty schists which are altered chloritic greenschists that occur in the ridge directly east of the fault. An increase in brecciation within bordering green phyllites and mafic volcanic rocks was noted towards the fault zone. A degraded Quaternary scarp is present along the southern end of the fault, but was not visited.

### 6.2. Tsetseg Thrust

The Tsetseg thrust scarp was observed from a distance and previously reported by Cunningham et al. (1996b). The scarp cuts the upper reaches of several prominent alluvial fans in the Tsetseg basin (Fig. 5b). Thrusting motion is interpreted based on prominent thrust sense kink bands in the adjacent phyllitic country rocks, the kilometre-high topographic escarpment along the fault and because most other Cenozoic thrust faults in the region are northwest striking.

### 6.3. Dariv Basin Scarp

The thrust fault shown in Fig. 6b, which is found at the top of the bajada along the west side of the Dariv Basin (Fig. 3), was examined and found to be expressed as a mature degraded scarp with a surface slope of 12° compared to a fan slope of 7° above and below the scarp. The scarp is 20 m high and small ephemeral streams have incised steep channels directly above the scarp suggesting forced fluvial downcutting on the upper plate with continued west-side uplift. Several large stream channels that cross the scarp show evidence for abandonment of older stream terraces with progressive downcutting (T1–T3 in Fig. 6b). It is suspected that each downcutting event coincided with a thrust earthquake on the fault. The fault cuts volcanic basement and Quaternary alluvium along the front and appears to link along strike with another degraded scarp that bounds the southern Dariv basin foreberg (Fig. 3). Thus the western margin of the Dariv Basin is interpreted to be bounded by an active basin-directed thrust fault that is overlapped by the extensive alluvial deposits shed off the southeastern ridge of the Sutai range.

## 7. Discussion

The Sutai range has bilateral structural vergence with western faults dipping eastwards into the range and eastern faults dipping westward into the range. These major structures bound discrete blocks with the deepest and highest-grade rocks exhumed in the centre of the range between the Tonhil Fault and the Central Thrust (Figs. 3, 8 and 10). It is unclear how much exhumation of metamorphic basement is due to Cenozoic thrusting and erosion and how much is due to pre-Cenozoic events. However, if the summit plateau represents a preserved regional peneplain of Cretaceous-Palaeocene age as occurs elsewhere in the Altai (Devyatkin, 1974) then only a maximum of 3

km of topographic uplift can be attributed to Cenozoic deformation (maximum relief of offset peneplain in region is approximately 3 km) and much of the exhumation of metamorphic basement within the range must be Pre-Cenozoic. Overall, simple extrapolation of surface fault attitudes to depth suggests that the cross-strike structure of the central and southern part of the range is an asymmetric positive flower structure rooted into the Tonhil fault (Fig. 11). This conclusion is also supported by the published section across the northern end of the range by Cunningham et al. (1996b) which shows outward directed thrust faults there. The western thrusts such as the Tsetseg and Upper Thrust appear to be the dominant structures responsible for an overall NE tilt to the range as reflected in modern-day stream length asymmetries within the range and the major topographic escarpment present along the Tsetseg fault (Figs. 3 and 5b). This fundamental structural and topographic asymmetry is probably due to the dominant NW-striking, NE dipping pre-existing structural grain within basement greenschists which was favourably oriented for brittle Cenozoic reactivation.

An evolutionary model is proposed for the range which involves step-by step development of the restraining bend taking into account development of faults, progressive shearing and vertical-axis rotations, pre-existing basement grain, progressive along-strike and across-strike growth of the range, and the role of forebergs in range growth (Fig. 12). Because initial segmentation is typical of strike-slip fault development (Wilcox et al., 1973; An and Sammis, 1996), it is assumed that the Tonhil Fault also was initially segmented and that a large stepover zone existed at the site of the future Sutai range. This is supported by palaeocurrent data from the Dzereg basin indicating that the first arrival of Oligocene-Miocene sediments was from the Sutai range thereby suggesting that the Sutai range was the earliest node of Late Tertiary uplift and erosion in the

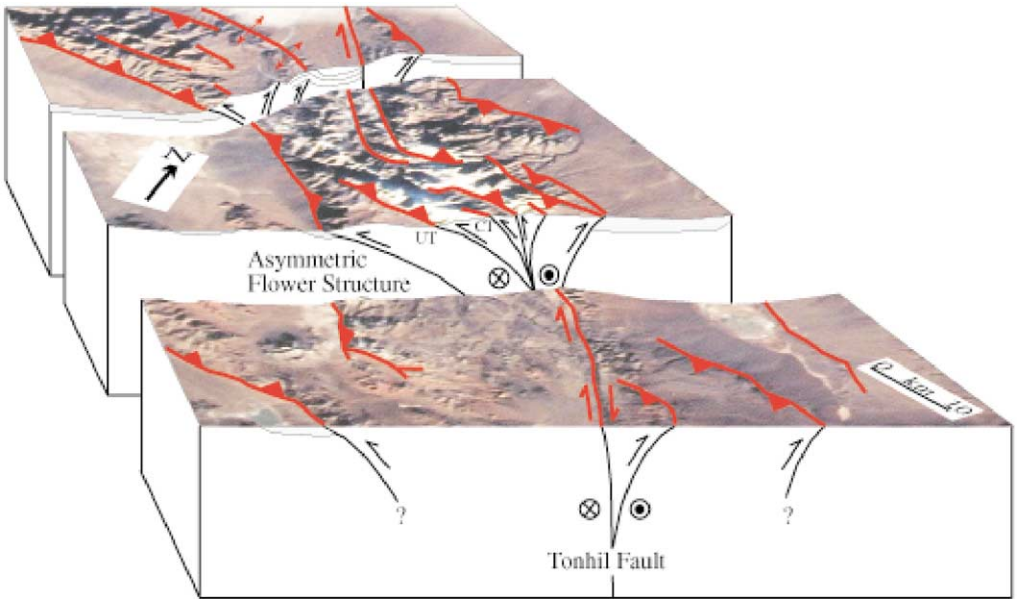


Fig. 11. Block diagram interpretation of fault geometries within Sutai Uul restraining bend. Downward extrapolation of major faults based on dips measured at surface suggests an overall asymmetric flower structure geometry within the core of the range. UT: Upper Thrust; CT: Central Thrust.

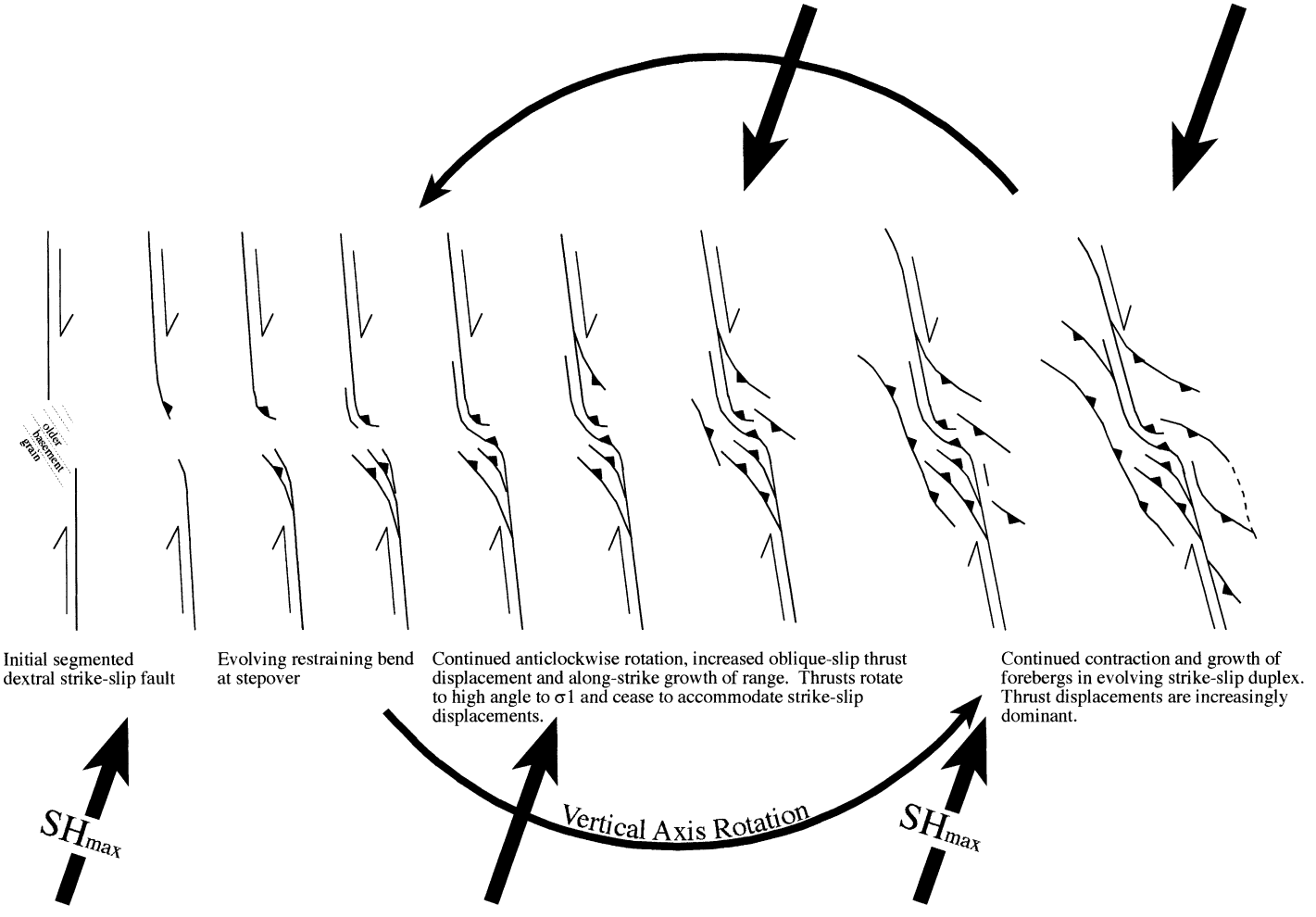


Fig. 12. Evolutionary model for Sutai Uul restraining bend. Initial segmented dextral strike-slip fault links through compressional P-shears at stepover, possibly due to intersection and linkage of horsetail splays at ends of strike-slip fault segments. With progressive displacements, some P-shears rotate to high angle with respect to σ1 and can no longer accommodate strike-slip displacements. Continued strike-slip displacements with a component of compression across the range lead to along-strike range growth, increased thrust-related uplift, strike-slip duplex fault geometries and anticlockwise rotation of blocks and bounding faults. Continued anticlockwise rotation of entire system relative to constant NE-directed SHmax increasingly promotes thrust displacements. Strike-slip displacements are increasingly subordinate because faults are at higher angle to σ1. With continued contraction, new thrust faults break out defining forebergs in surrounding basins which eventually link as part of evolving transpressional duplex.

region (Howard et al., 2003). The model suggests that a continuous NE-directed maximum horizontal stress (derived from the continued Late Tertiary indentation of India into southern central Asia to the south; Tapponnier and Molnar, 1979; Zoback, 1992) was the driving force for progressive dextral displacements and NE or SW-directed thrusting. The pre-existing northwest striking Altai basement grain may have influenced initial strike-slip fault segmentation and location of stepover zones. Blocks and the faults that bound them rotated in an anti-clockwise sense with progressive displacements consistent with regional oroclinal bending at the southeastern end of the Altai and basic geometrical considerations of displacement transfer at strike-slip fault terminations (Cunningham et al., 1996a,b, 2003; Bayasgalan et al., 1999). Strike-slip faults terminating in thrust faults and oblique-slip thrusts rotated to an orientation less favourable for further strike-slip displacements which prompted new strike-and oblique-slip splays to develop enabling the range to grow along-strike (Fig. 12). With progressive anti-clockwise crustal rotation, the strike-slip faults became subordinate structures to the NW-striking thrust faults which increasingly accommodated the majority of the NE-directed horizontal stress. In this way, the original strike-slip faults along which the range nucleated were increasingly overprinted and obscured, especially in the core of the range and original stepover zone, whereas they are still visible and potentially active at the northwest and southeast ends of the range. With continued compression across the range, new forebergs developed to accommodate some of the crustal shortening which led to widening of the range. The forebergs may have also rotated and linked to form an incipient strike-slip duplex as is observed in the western Dariv basin adjacent to the Sutai range (Figs. 2 and 3).

Both sides of the Sutai range are active sites of faulting and range growth as indicated by the Tsetseg and Dariv basin scarps (Figs. 2, 3, 5 and 6). In addition, the Tonhil Fault and Upper and Central Thrusts all appear as sharp topographic breaks with very low mountain front sinuosity and are therefore likely sites of Quaternary movement. Thus at least five major faults within and bounding the Sutai range are likely to have experienced Quaternary activity and pose a potential seismic risk. The deeply incised canyons in the centre of the range and upwarped gangplank surfaces suggest that the central fault blocks are susceptible to continued thrust-related uplift. Total minimum shortening across the range is approximately 5 km based on a maximum of 3 km of peneplain uplift for the summit block on moderately dipping bounding faults and minimum shortening estimates for the other major faults along transect A–F (Figs. 3 and 8).

The role of pre-existing faults in influencing the fundamental Cenozoic fault geometry of the range is uncertain. The ductile l-tectonites in the core of the range may suggest reactivation of an older strike-slip zone there. The Dariv and Dzereg Basins contain Mesozoic sediments and inverted Mesozoic normal faults are interpreted from the Dzereg Basin (Howard et al., 2003). Although the Sutai range lacks inverted basin fill within the range itself, Mesozoic clastic sediments do occur in the marginal forebergs suggesting that foreberg growth and fault linkage may relate to normal fault inversion. The overall importance of fault reactivation and inversion within intramontane and flanking basins of the Mongolian Altai is at present difficult to assess without seismic reflection data.

The Sutai range is a natural testing ground for Keller et al.'s (1997) and McClay and Bonora's (2001) analog models of restraining bend development. Major faults that splay off of the Tonhil Fault such as the Upper and Central Thrust are essentially P-shears consistent with Keller et al.'s (1997) models. The overall fault geometries within the Sutai range are most consistent with model

experiments where the initial strike-slip faults underlap (McClay and Bonora, 2001). However, the clay box and sandbox models do not allow for regional block rotation within a constant stress field which results in changing kinematics along rotating faults. In addition, the Sutai range formed in crust with a NW-striking basement grain which may have been a first-order influence on P-shear localization, fault dip and thus kinematics (Fig. 12). It is clear that when attempting to understand natural examples of restraining bends, multiple factors will influence the fault geometry and structural and geomorphic evolution of the range including: the initial width of the stepover zone and degree of strike-slip fault overlap, the attitude of pre-existing crustal fabrics (e.g. schistosity), the presence of pre-existing weak faults susceptible to reactivation, the direction of SHmax relative to the basement structures, and the likelihood of progressive block and fault rotation through time on a regional scale and within the bend itself.

## Acknowledgements

D. Cunningham was supported by Royal Society Grant No. 22077.

## References

An, L.-J., Sammis, C.G., 1996. Development of strike-slip faults: shear experiments in granular materials and clay using a new technique. Journal of Structural Geology 18 (8), 1061–1077.

Anderson, R.S., 1990. Evolution of the northern Santa Cruz mountains by advection of crust past a San Andreas Fault bend. Science 249, 397–401.

Badarch, G., Cunningham, D., Windley, B., 2002. A new terrane subdivision for Mongolia: implications for the Phanerozoic crustal growth of Central Asia. Journal of Asian Earth Sciences 21, 87–110.

Baljinnyam, I., Bayasgalan, A., Borisov, B.A., Cisternas, A., Dem'yanovich, M.G., Ganbataar, L., Kochetkov, V.M., Kurushin, R.A., Molnar, P., Hervé, P., Vashchilov, Yu.Ya., 1993. Ruptures of major earthquakes and active deformation in Mongolia and its surroundings. Boulder, Colorado, Geological Society of America Memoir 181.

Barka, A.A., Kadinsky-Kade, K., 1988. Strike-slip fault geometry in Turkey and its influence on earthquake activity. Tectonics 7 (3), 663–684.

Bayasgalan, A., Jackson, J., Ritz, J.-F., Carretier, S., 1999. Field examples of strike-slip fault terminations in Mongolia and their tectonic significance. Tectonics 18 (3), 394–411.

Biddle, K.T. & Christie-Blick, N., 1985, Glossary-strike-slip deformation, basin formation and sedimentation. In: Biddle, K.T., Christie-Blick, N. (eds.), Strike-slip deformation, Basin Formation and Sedimentation. SEPM Special Publication 37, 375–384.

Blythe, A.E., Burbank, D.W., Farley, K.A., Fielding, E.J., 2000. Structural and Topographic evolution of the central Transverse Range, California, from apatite fission-track, (U-Th)/He and digital elevation model analyses. Basin Research 12 (2), 97–114.

Butler, R.W.H., Spencer, S., Griffiths, H.M., 1998, The structural response to evolving plate kinematics during transpression: evolution of the Lebanese restraining bend of the Dead Sea Transform, In: Holdsworth, R.E., Strachan, R.A., Dewey, J.F. (Eds.), Continental Transpressional and Transtensional Tectonics. Geological Society, London, Special Publications, 135, 81–106.

Chen, B., Bor-Ming Jahn, 2002. Geochemical and isotopic studies of the sedimentary and granitic rocks of the Altai orogen of northwest China and their tectonic implications. Geological Magazine 139 (1), 1–13.

Crowell, J.C., 1974, Sedimentation along the San Andreas fault, California, in Dott, R.H., Jr., and Shaver, R.H., eds.,

Modern and Ancient Geosynclinal Sedimentation: Society of Economic Palaeontologists and Mineralogists Special Publication No. 19, 292–303.

Crowell, J.C., 1979. The San Andreas fault through time. Journal of Geological Society London 136, 292–302.

Cunningham, W., 1995. Dickson, Orogenesis at the southern tip of the Americas: the structural evolution of the Cordillera Darwin metamorphic complex, southernmost Chile. Tectonophysics 244 (4), 197–229.

Cunningham, W., Dickson, Windley, Brian, F., Dorjnamjaa, D., Badamgarov, G., Saandar, M., 1996a. Late Cenozoic transpression in southwestern Mongolia and the Gobi Altai-Tien Shan connection. Earth and Planetary Sciences 140 (1-4), 67–82.

Cunningham, W.D., Windley, B.F., Dorjnamjaa, D., Badamgarov, G., Saandar, M., 1996b. structural transect across the Mongolian Altai: active transpressional mountain building in central Asia. Tectonics 15 (1), 142–156.

Cunningham, W.D., 1998. Lithospheric controls on late Cenozoic construction of the Mongolian Altai. Tectonics 17 (6), 891–902.

Cunningham, D., Dijkstra, A., Howard, J. Quarles, A., Badarch, G., 2003. Active intraplate strike-slip faulting and transpressional uplift in the Mongolian Altai. In: Intraplate Strike-slip Deformation Belts, Special Volume of the Geological Society of London.

Devyatkin, E.V., 1974, Structures and formational complexes of the Cenozoic activated stage. In: Tectonics of the Mongolian People's Republic. Moscow, Nauka, 182–195. (in Russian).

Devyatkin, E.V., 1981, The Cenozoic of Inner Asia Stratigraphy, (geochronology and correlation. In: Nikiforova, K. V. (Ed.), Combined Soviet-Mongolian Scientific Research Geoogical. Expedition Transactions, 27, Nauka, Moscow (in Russian).

Dumitru, T.A., Zhou, D., Chang, E.Z., Graham, S.A., Hendrix, M.S., Sobel, E.R., Carroll, A.R., 2001, Uplift, exhumation and deformation in the Chinese Tian Shan, In: Hendrix, M.S., Davis, G.A. (Eds.), Paleozoic and Mesozoic evolution of central Asia: From continental assembly to intracontinental deformation: Boulder, Colorado, Geological Society of America Memoir 194, 117-149.

Gavrilova, S.P., 1975. Granitoid formations of Western Mongolia. Granitoid and alkaline formations in the structures of Western and Northern Mongolia. Transactions, Moscow, Nauka 14, 50–143.

Hendrix, M.S., 2000. Evolution of Mesozoic sandstone compositions, southern Junggar, northern Tarim, and western Turpan basins, northwest China: a detrital record of the ancestral Tian Shan. Journal of Sedimentary Research 70 (3), 520–532.

Howard, J.P., Cunningham, W.D., Davies, S.J., Dijkstra, A.H., Badarch, G., 1993. The stratigraphic and structural evolution of the Dzereg Basin, Western Mongolia: Clastic sedimentation, fault inversion and basin destruction in an intracontinental transpressional setting. Basin Research 15, 45–72.

Kadinsky-Cade, K., Barka, A. A. 1989. Effects of restraining bends on the rupture of strike-slip earthquakes. In: David P. Schwartz and Richard H. Sibson (Eds.) Proceedings of Conference XLV on Fault Segmentation and Controls of Rupture Initiation and Termination, USGS Open-File Report 89-315, pp. 181–192.

Keller, J.V.A., Hall, S.H., McClay, K.R., 1997. Shear fracture pattern and microstructural evolution in transpressional fault zones from field and laboratory studies. Journal of Structural Geology 19 (9), 1173–1187.

Khil'ko, S.D., Kurushin, R.A., Kochetkov, V.M., Baljinnyam, I., Monkoo, D., 1985. Earthquakes and the bases for seismic zoning of Mongolia. Transactions 41, The joint Soviet-Mongolian Scientific Geological Research Expedition, Moscow, Nauka 215.

Laney, S., Gates, A.E., 1996. Three-dimensional shuffling of horses in a strike-slip duplex: an example from the Lambert sill, New Jersey. Tectonophysics 258, 53–70.

Legg, M., 2000. Development and growth of large transpressional stopovers in strike-slip faults; seismotectonics of major restraining bends along strike-slip faults, 2000 AAPG Pacific Section and Western Region Society of Petroleum Engineers Meeting, abstracts. AAPG Bulletin no 6, 880–881.

Mann, P., Draper, G., Burke, K., 1985. Neotectonics of a strike-slip restraining bend system, Jamaica. In: Biddle, K.T., Christie-Blick, N. (Eds.), Strike-Slip Deformation, Basin Formation and Sedimentation. SEPM Special Publication, pp. 211–226.

Mann, P., Burke, K., Matumoto, T., 1984. Neotectonics of Hispaniola: plate motion, sedimentation, and seismicity at a restraining bend. Earth and Planetary Science Letters 70, 311–324.

McClay, K., Bonora, M., 2001. Analog models of restraining stepovers in strike-slip fault systems. AAPG Bulletin 85 (2), 233–260.

Mossakovsky, A.A., Ruzhentsev, S.V., Samygin, S.G., Kheraskova, T.N., 1994. Central Asia fold belt: Geodynamic evolution and formation history. Geotectonics 27, 445–474.

Schwartz, S.Y., Orange, D.L., Anderson, R.S., 1990. Complex fault interactions in a restraining bend on the San Andreas Fault, southern Santa Cruz Mountains, California. Geophysical Research Letters 17, 1207–1210.

Sjostrom, D.J., 2001, Sedimentology and provenance of Mesozoic nonmarine strata in western Mongolia: a record of intracontinental deformation. In: Hendrix, M.S., Davis, G.A. (Eds.), Palaeozoic and Mesozoic Tectonic Evolution of Central and Eastern Asia: From Continental Assembly to Intracontinental Deformation, Geol. Soc. Am. Memoir, 194, 361–388.

Tapponnier, P., Molnar, P., 1979. Active faulting and Cenozoic tectonics of the Tien Shan, Mongolia, and Baykal regions. Journal of Geophysical Research 84, 3425–3459.

Wilcox, R.E., Harding, T.P., Seely, D.R., 1973. Basic wrench tectonics. American Association of Petroleum Geologists Bulletin 57 (1), 74–96.

Windley, B.F., Kröner, A., Guo, J., Qu, G., Li, Y., Chi Zhang, 2002. Neoproterozoic to Paleozoic geology of the Altai orogen, NW China: new zircon age data and tectonic evolution. Journal of Geology 110, 719–737.

Woodcock, N., Fisher, M., 1986. Strike-slip duplexes. Journal of Structural Geology 8, 725–735.

Zaitsev, N.S., 1978. Geological Map of the Mongolian Altai, 1:500,000 scale. Acad. Sci., USSR, Acad. Sci., Mongolian People's republic, Comb. Sov-Mongolian Sci. Res. Geol. Exped., Nauka, Moscow. (in Russian).

Zoback, M.L., 1992. First- and second- order patterns of stress in the lithosphere: The world stress map project. Journal of Geophysical Research 97 (B8), 703–711,728.